3 November 2000

ELSEVIER

Chemical Physics Letters 330 (2000) 34–40

CHEMICAL PHYSICS LETTERS

www.elsevier.nl/locate/cplett

Electron and positron scattering from CF_3I molecules below 600 eV: a comparison with CF_3H

Michihito K. Kawada, Osamu Sueoka, Mineo Kimura *

Graduate School of Science and Engineering, Yamaguchi University, Ube 755-8611, Japan

Received 12 April 2000; in final form 21 September 2000

Abstract

The total cross-sections (TCSs) for electron and positron scattering from CF_3I molecules have been studied experimentally. A theoretical analysis based on the continuum multiple-scattering (CMS) method has been performed to understand the origin of resonances and the elastic cross-sections. The present TCS for electron scattering is found to be larger by about 20% than that of T. Underwood-Lemons, D.C. Winkler, J.A. Tossel, J.H. Moore [J. Chem. Phys. 100 (1994) 9117] although the general shape agrees well in the entire energy studied. The difference in the cross-sections for CF_3I and CF_3H is explained by the sizes and the dipole moments of these molecules.

1. Introduction

Perfluorocarbon (C_mF_n) molecules have been regarded as important and efficient gases for plasma etching over the years and used extensively in semiconductor manufacturing industries [1]. For environmental reasons, however, the use of perfluorocarbons will be terminated in the near future. Trifluoromethyl iodide is considered as an alternative etching gas replacing perfluorocarbons, because the C–I bond is known to be readily breakable releasing CF_3 radicals [2] for etching. To assess the behavior of this molecule in the plasma environment, it is crucial to understand its spectroscopic properties and dynamics, particularly electron scattering cross-sections at low to intermediate energies. Furthermore, a comparative study using electron and positron impact should contribute to a better understanding of the interaction and dynamics of these systems.

Therefore, we conducted a parallel study of electron and positron scattering from CF_3I for total cross-sections (TCSs) and elastic cross-sections for providing benchmark data, on which no reliable and comprehensive data are yet available to the best of our knowledge. The TCSs for CF_3X and CF_2X_2 (X = Cl, Br and I) by electron impact in the region of 0.3–12 eV were measured by Underwood-Lemons et al. [3]. They observed resonance peaks in their TCSs for all molecules and interpreted them as electron attachment into one of the unoccupied molecular orbitals (UMOs). Oster et al. [4] studied the temporary negative ion formation induced by low-energy electron impact to CF_3I and observed two structures assignable to dissociative attachment (DA) at ≈0 and 3.8 eV. This negative ion undergoes further breaking-up

* Corresponding author. Fax: +81-836-85-9801.
E-mail address: mineo@po.cc.yamaguchi-u.ac.jp (M. Kimura).

0009-2614/00/$ - see front matter
PII: S0009-2614(00)01095-2

Table 1
Molecular properties

	Number of valence electrons	Electronic configuration	Bond length (Å)	Dipole moment (D)
CF_3I	32	$\ldots(4a_1)^2(4e)^4$	2.14 (C–I), 1.33 (C–F)	1.048
CF_3H	26	$\ldots(1a_2)^2(6a_1)^2$	1.10 (C–H), 1.33 (C–F)	1.651

and may yield a negative ion fragment and a radical.

Recently, we measured the TCSs for electron and positron scattering from CF_3H and discussed the similarity and difference in the dynamics of CH_4 and CF_4 molecules [5]; this difference implied that interactions and dynamics of scattering are affected by molecular properties. Now we have extended the measurements of TCSs for CF_3I in a wide range of impact energy (0.7–600 eV), which are compared with the TCSs of CF_3H [5] to study the effect of dipole moment and molecular size on TCSs. The molecular properties that have possible influence on the TCSs are listed in Table 1.

2. Experimental and theoretical methods

2.1. Experimental

The linear transmission method has been used to measure the absolute TCS for positron and electron scattering from CF_3I molecules. The apparatus has been reported in [6,7]. Variable-energy positron or electron beams were produced from an annealed tungsten moderator placed in front of a ^{22}Na radioisotope ($\approx$100 μCi). The energy widths of the positron and electron beams were $\approx$1.5 and 1 eV, respectively. The beam passing through a collision cell was transported to a detector by a magnetic field. The projectile-beam intensities, I_g and I_v, were obtained by the time-of-flight spectra with and without the target of a number density n in the collision cell, respectively. The TCS values Q_t were derived from

$$Q_t = -\frac{1}{nl}\ln\left(\frac{I_g}{I_v}\right), \tag{1}$$

where l is the effective length of the collision cell, established by normalizing the TCSs to those in the positron–N_2 data of Hoffman et al. [8]. The electron energy was gauged to the positions of resonances for N_2, CO and CO_2 molecules, while for the positron energy, no tuning of the energy was made. The pressure independence of the TCS of CF_3I was confirmed by electron scattering at 6 and 27 eV.

Correction was made to derive quantitative TCSs for the acceptance of the detector of positrons or electrons scattered in the small-angle forward direction in the collision cell, as described in detail previously [9]. The correction for electron scattering amounted to 10–18% below 30 eV, but much smaller at higher energies, to <5% above 100 eV. The correction for positron scattering was in general slightly larger. The sum of all uncertainties, $\Delta I/I$, $\Delta n/n$ and $\Delta l/l$, was estimated to be 3–5% for electrons and 4.5–6.5% for positron scattering. The purity of the CF_3I gas was 97%.

2.2. Theoretical model

The theoretical approach employed is the continuum multiple-scattering (CMS) method; this is a simple but efficient model for treating electron scattering from polyatomic molecules [10]. To overcome difficulties arising from (1) the many degrees of freedom of electronic and nuclear motions and (2) the non-spherical molecular field in a polyatomic molecule, the CMS divides the configuration space into three regions: atomic, interstitial and outer. The scattering part of the method is based on the static-exchange-polarization potential model within the fixed-nuclei approximation. The static interaction is constructed by the electron density obtained from the CMS wave function, and the Hara-type free-electron gas model [10] is employed for the local-exchange interaction, while the dipole interaction is considered only for terms proportional to r^{-2}, where r denotes the distance of the incident electron from the center of mass of the molecule.

Under these assumptions, the Schrödinger equation in each region is solved numerically under separate boundary conditions. By matching the wave functions and their derivatives from each region, one can determine the total wave functions of the scattered electron, and hence the scattering **S**-matrix and cross-sections, by a conventional procedure. The CMS has been tested extensively and is known to provide useful information on the underlying scattering physics [11]. Note that the CMS is applied in the present calculation to electron scattering only, because the electron–molecule interaction can be approximately described.

3. Results

We discuss below the TCSs for electron and positron impacts separately. In addition, a detailed comparison with the CF_3H molecule is described to clarify the spectroscopic dynamical aspects of the CF_3I molecule.

3.1. Electron impact

The TCSs for electron scattering from CF_3I obtained for 0.8–600 eV are shown in Fig. 1. The numerical values are given in Table 2.

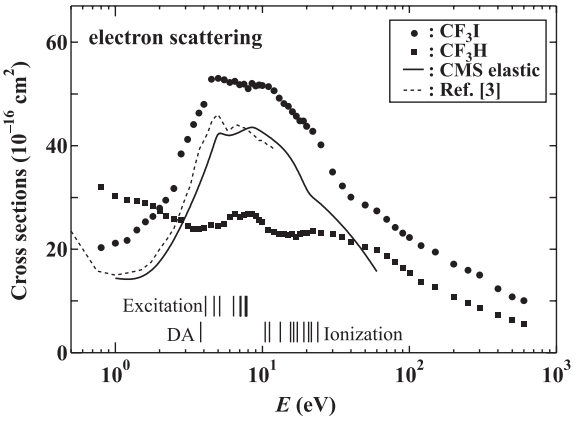

Fig. 1. Electron scattering TCSs: (●) CF_3I, present study; (■) CF_3H [5]; (- - -) CF_3I [3]; (—) elastic scattering cross-section for CF_3I, present theoretical study. The vertical lines mark the thresholds for excitation and ionization states and the resonance energy for DA for CF_3I (see Table 3).

The TCS for the CF_3I measured earlier by Underwood-Lemons et al. [3] based on electron transmission spectroscopy is included in Fig. 1. Two peaks around 5 and 7 eV are clearly discriminated in their data, whereas the present data show a single broad peak with small structures at corresponding energies, because their energy resolution is higher than ours. The energy dependence of their TCSs agrees with the present measurement within experimental error. However, the magnitude of their TCS is found to be smaller by ≈20% than that of the present TCS in the entire energy range studied; this difference may be ascribed to underestimation of the forward scattering effect in their TCS.

We have calculated the electronic structure based on the Hartree–Fock method, in which the results can be compared with those of large-scale calculations within 15% [3]. Our calculation suggests that two UMOs of a_1 symmetry are located at 4.32 and 8.87 eV relative to the ionization edge. These values correspond with the previous estimation [3]. The observed large peak centered at 6 eV can be assigned to the combination of these UMOs. Above 12 eV, the small structure observed around 25 eV is assigned to the combination of several UMOs with different symmetries. The elastic cross-sections calculated by CMS are also shown in Fig. 1. The energy dependence of the cross-section is similar to the present TCS, but the magnitude is smaller by 20–30%. The difference between the TCS and the elastic cross-section accounts for contributions from other inelastic processes.

The transition energies to four electronic excitation bands (the so-called A, B, C and D bands) of CF_3I were measured [12–14]; the bands lie around 4.5–7.5 eV above the ground state, on the lower side of the large peak located at 4–11 eV. Relevant electron binding energies [15] and excitation bands are listed in Table 3. Since the DA due to resonances is known to occur around ≈0 and 3.8 eV [4], the 3.8 eV-resonance may somehow participate in the peak in the present region. The excitation and DA play an important role for producing various radicals from CF_3I, because the $^3Q_0$ state in the A band [12] dissociates to produce excited I^* atom, as reported by a photodissociation

Table 2
The TCSs (10^{-16} cm^2) of CF_3I by electron and positron impacts

eV	Electron	Positron
0.7	–	14.6 ± 0.9
0.8	20.3 ± 0.8	–
1.0	21.2 ± 0.8	15.9 ± 0.9
1.2	21.7 ± 0.8	–
1.3	–	18.0 ± 1.1
1.4	23.7 ± 0.8	–
1.6	25.3 ± 0.9	19.7 ± 1.2
1.8	26.3 ± 0.9	–
1.9	–	22.4 ± 1.2
2.0	27.9 ± 1.0	–
2.2	29.5 ± 1.1	22.9 ± 1.2
2.5	31.7 ± 1.3	22.8 ± 1.1
2.8	38.4 ± 1.4	22.3 ± 1.2
3.1	41.2 ± 1.5	23.2 ± 1.3
3.4	44.1 ± 1.7	24.7 ± 1.3
3.7	46.3 ± 1.9	24.6 ± 1.3
4.0	48.0 ± 2.0	24.9 ± 1.2
4.5	52.8 ± 2.0	27.0 ± 1.4
5.0	53.0 ± 2.0	28.6 ± 1.5
5.5	52.7 ± 2.1	28.4 ± 1.5
6.0	52.2 ± 2.2	29.3 ± 1.6
6.5	52.4 ± 2.2	28.3 ± 1.6
7.0	51.8 ± 2.4	29.7 ± 1.7
7.5	51.9 ± 2.3	29.7 ± 1.6
8.0	51.0 ± 2.5	28.3 ± 1.5
8.5	52.0 ± 2.7	28.0 ± 1.4
9.0	51.6 ± 2.4	28.3 ± 1.5
9.5	51.7 ± 2.2	28.3 ± 1.4
10.0	51.6 ± 2.1	27.4 ± 1.2
11	51.4 ± 1.8	27.3 ± 1.3
12	50.6 ± 1.9	27.8 ± 1.4
13	49.2 ± 2.0	27.3 ± 1.4
14	48.1 ± 2.2	26.9 ± 1.4
15	47.6 ± 2.1	27.7 ± 1.4
16	46.6 ± 2.2	27.9 ± 1.5
17	45.7 ± 2.1	27.7 ± 1.5
18	44.8 ± 2.2	27.8 ± 1.6
19	44.8 ± 2.0	27.5 ± 1.5
20	43.8 ± 1.9	27.7 ± 1.5
22	42.8 ± 1.9	27.0 ± 1.3
25	40.2 ± 1.7	26.4 ± 1.4
30	34.9 ± 1.7	25.8 ± 1.2
35	32.2 ± 1.5	–
40	30.1 ± 1.4	25.2 ± 1.2
50	28.5 ± 1.2	23.2 ± 1.1
60	27.4 ± 1.1	22.8 ± 1.3
70	25.8 ± 1.0	20.3 ± 1.2
80	24.2 ± 1.0	22.0 ± 1.0
90	23.1 ± 0.9	20.8 ± 1.1
100	22.3 ± 0.9	20.5 ± 1.0
120	20.7 ± 0.8	19.6 ± 1.0
150	19.4 ± 0.7	18.0 ± 0.9
200	17.1 ± 0.6	16.0 ± 0.9
250	15.9 ± 0.6	14.7 ± 0.8
300	15.0 ± 0.5	13.5 ± 0.8
400	12.4 ± 0.4	12.3 ± 0.8
500	10.8 ± 0.3	10.9 ± 0.7
600	10.1 ± 0.3	9.7 ± 0.6

study [16], and the DA at ≈3.8 eV is known to lead to fragments such as $CF_3^- + I$, $CF_2I + F^-$ and $CF_2 + FI^-$ [4].

Hence, the main contribution to this large peak is the shape resonance attributed to temporary capture in UMOs, superimposed by a small contribution from the DA around 3.8 eV. As the energy increases, the transition to the four excited states gradually increases from each threshold. In this domain below the threshold, the difference between the TCS and elastic cross-section may substantially be contributed by ro-vibrational excitation cross-sections except in the region of the DA.

The TCS continues to fall below 4 eV before it turns around and start to increase at a much lower energy, because CF_3I is a polar molecule (see Table 1). For a polar molecule, the cross-section is known to increase nearly inversely to the energy at lower energies. Underwood-Lemons et al. [3] found a minimum around 1 eV and termed it the Ramsauer–Townsend (RT) minimum. It is questionable, however, to regard it as a RT minimum, since the target is a polar-molecule and hence the potential may be too attractive to cause it according to our CMS analysis.

At the high-energy side, the decreasing trend of the TCS becomes somewhat weaker around 40 eV and a weak shoulder is seen at ≈70 eV. Generally, the ionization process shows a rapid growth from the threshold to ≈100 eV; the total ionization cross-section of 10.9×10^{-16} cm^2 [17] measured around 70 eV amounts to about 42% of our TCS.

The aspects arising from the electronic structures and resonances in TCSs for CF_3I are compared with those for CF_3H [5]. The TCSs for CF_3H, included in Fig. 1, have a relatively strong peak around 7–8 eV with a second broad peak centered at 25 eV. These peaks are dominantly assigned to shape resonances of t_2 and e symmetries

Table 3
Binding energy of the occupied valence molecular orbitals and transition energy of the electronic excited states of CF_3I

Occupied MOs	Binding energy [a] (eV)	Excited state	Transition energy (eV)
4e	10.45, 11.18[b]	A	4.7[c]
$4a_1$	13.25	B	6.4[d]
$1a_2$	15.56	C	7.1[d]
3e	16.32	D	7.7[d]
2e	17.28		
$3a_1$	19.15		
1e	20.6		
$2a_1$	21.5		
$1a_1$	23.8		

[a] Photoelectron spectroscopy [15].
[b] Split by spin-orbit coupling [15].
[c] The $^3Q_0$ state by magnetic circular dichroism spectroscopy [12].
[d] The lowest state by $(2+1)$ resonance-enhanced multiphoton ionization spectroscopy [14].

[5], similar to that for CF_3I. Contrary to CF_3I, however, the TCS continues to increase below 3 eV, which is a clear manifestation of the strong dipole moment of CF_3H (see Table 1).

3.2. Positron impact

The TCSs for positron impact are displayed in Fig. 2 along with those for CF_3H [5]. In the 2–3 eV range, the TCS has a step-like structure attributable to the opening of a new positronium (Ps) formation channel with its threshold at 3.65 eV. This threshold behavior appears to be broadened by the limited energy resolution of the present experiment. A few structures, also observed between 3 and 20 eV, are attributable to the opening of new channels for a series of electronic excitation in $\geqslant$4.7 eV and direct ionization at 10.45 eV. Other weak structures appear in the entire region.

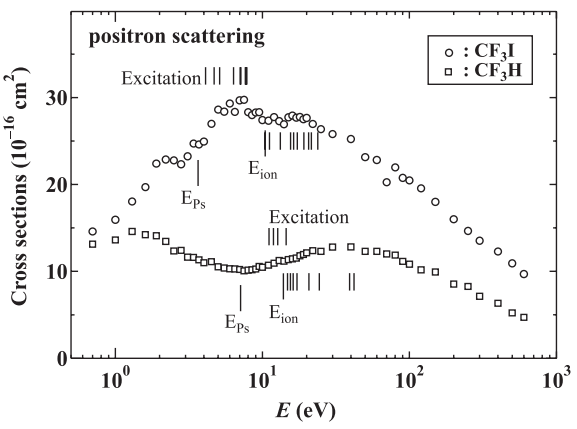

Fig. 2. Positron scattering TCSs: (○) CF_3I, present study; (□) CF_3H [5]. The vertical lines mark the thresholds for excitation and ionization states and Ps for CF_3I (see Table 3) and CF_3H [19].

The present TCSs are compared with those for CF_3H. For CF_3H [5], the TCSs show two large peaks centered at 1.5 and above 20 eV, but the first peak is completely missing in CF_3I. The origin of the peak for CF_3H at 1.5 eV is still unknown, but it is likely to be due to larger ro-vibrational excitation cross-sections, similar to the CO_2 case [18]. The thresholds for electronic excitation, $>$11 eV [19], and the Ps formation, $\approx$6.9 eV, are higher than this peak energy. The peak beyond 20 eV, attributed to a combination of ionization, Ps formation, and electronic excitations for CF_3H, is similar to a small shoulder around 40 eV for CF_3I. The TCS for CF_3I is larger by a factor of two to three than that for CF_3H from a few eV to 50 eV. This is partly because of lower thresholds for electronic excitation and ionization for CF_3I and availability of more channels of electronic excitation.

A broad maximum, which is missing in the case of CF_3H, can be seen from the threshold Ps formation to that of ionization in the TCS for the CF_3I. This difference is due to the excitation cross-sections and maybe that of Ps formation. The mechanism of Ps formation may be related closely to interaction of a number of valence electrons and

their angular momenta between two molecules (see Table 1). Our measurement of the ratio of the Ps formation cross-section to the TCS at 2 eV above the respective thresholds for both molecules, indicate that the ratio is about 10% and 5.9% for CF_3I and CF_3H, respectively [20]. The larger contribution of the Ps formation to the TCS for CF_3I is attributable, in part, to a larger number of electrons available.

Above 50 eV, the ratio of the TCSs for CF_3I to CF_3H is roughly constant, 1.9. Incidentally, this value is found to be nearly equivalent to the ratio of the molecular size. The charge distributions of these molecules change along the C–I (≈2.1 Å) and C–H (≈1.1 Å) bonds. To the contrary, the ratio between the TCSs of electron scattering for CF_3I and CF_3H appears to increase from 1.5 to 1.8 with increasing electron energy from 50 to 600 eV. This indicates that for electron scattering, the static, exchange and dipole interactions are all interrelated in a more complex manner than that for positron scattering even in this energy domain.

3.3. A comparison of TCSs between electron and positron impacts

The TCSs for electron and positron impacts are plotted in Fig. 3. In the present entire impact-energy range, the TCSs for positrons are always smaller than those for electrons. At low to intermediate energies, the TCS for electron impact is always larger by nearly a factor of two due to the resonance at 3–30 eV region, and they appear to converge gradually beyond 100 up to 600 eV. Below 3 eV, the TCS for electron impact decreases sharply and approaches to that of positron impact. However, this trend of the cross-sections seems to be accidental. To confirm the influence of dipole moment, both TCSs should be studied at much lower energies than the present experimental limits, where the point of increase in the TCSs could be observed.

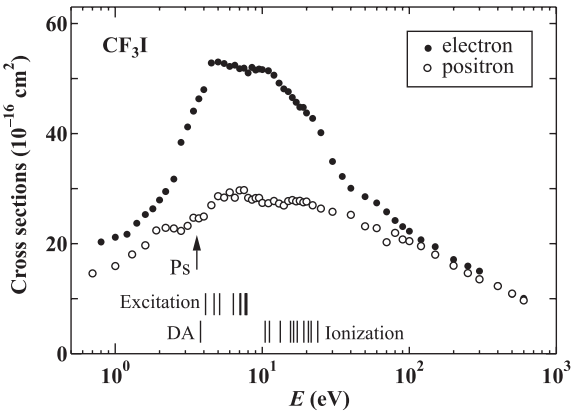

Fig. 3. Comparison of the TCSs for CF_3I by electron (•) and positron (○) scattering. The vertical lines mark the thresholds for excitation and ionization states and for Ps and the resonance energy for DA (see Table 3).

4. Summary

We present the experimental TCSs for CF_3I by electron and positron impacts from 0.7 to 600 eV. The TCSs for electrons are found to be consistently lager than the corresponding data of Underwood-Lemons et al. [3]. Theoretical results based on the CMS method provide information on the origin and positions of resonances and support the energy dependence and magnitude of the TCSs and the observed structures in the TCSs for electron impact. Using both projectiles, a comparative study of the TCSs for CF_3I and CF_3H, where a heavy or light atom is bonded to the trifluoromethyl group, provides insight into the interaction and dynamics. The observed trends in the TCSs for these molecules may be explained qualitatively in terms of their permanent electric dipole moments, $CF_3I < CF_3H$, at low energy and the bond length, C–I > C–H, at high energy. No information on the transition to electronically and ro-vibrationally excited states by positron impacts is yet available for understanding the scattering processes at intermediate energy region.

Acknowledgements

The work has been supported in part by a Grant-in-Aid, the Ministry of Education, Science, Sports and Culture, Japan, and by the grant from the National Institute for Fusion Science.

References

[1] L.C. Christophorou (Ed.), Electron–Molecule Interactions and their Applications, vol. 1, 2, Academic Press, New York, 1984.
[2] S. Samukawa, T. Mukai, in: Proceedings of the International Symposium on Electron–Molecule Collisions and Swarms, Tokyo, 1999, Abstract, p. 76.
[3] T. Underwood-Lemons, D.C. Winkler, J.A. Tossell, J.H. Moore, J. Chem. Phys. 100 (1994) 9117.
[4] T. Oster, O. Ingolfsson, M. Meinke, T. Jaffke, E. Illenderger, J. Chem. Phys. 99 (1993) 5141.
[5] O. Sueoka, H. Takaki, A. Hamada, H. Sato, M. Kimura, Chem. Phys. Lett. 288 (1998) 124.
[6] O. Sueoka, S. Mori, J. Phys. B 19 (1986) 4035.
[7] O. Sueoka, S. Mori, A. Hamada, J. Phys. B 27 (1994) 1453.
[8] K.R. Hoffman, M.S. Dababneh, Y.-F. Hsieh, W.E. Kauppila, V. Pol, J.H. Smart, T.S. Stein, Phys. Rev. A 25 (1982) 1393.
[9] A. Hamada, O. Sueoka, J. Phys. B 27 (1994) 5055.
[10] M. Kimura, H. Sato, Comments At. Mol. Phys. 26 (1991) 333.
[11] H. Tanaka, Y. Tachibana, M. Kitajima, O. Sueoka, H. Takaki, A. Hamada, M. Kimura, Phys. Rev. A 59 (1999) 2006.
[12] A. Gedanken, Chem. Phys. Lett. 137 (1987) 462.
[13] M.B. Robin, Can. J. Chem. 63 (1985) 2032.
[14] C.A. Taatjes, J.W.G. Mastenbroek, G. van den Hoek, J.G. Snijders, S. Stolte, J. Chem. Phys. 98 (1993) 4355.
[15] B.W. Yates, K.H. Tan, G.M. Bancroft, J. Chem. Phys. 85 (1986) 3840.
[16] H.J. Hwang, M.A. El-Sayed, J. Phys. Chem. 96 (1992) 8728.
[17] J.A. Beran, L. Kevan, J. Phys. Chem. 73 (1969) 3866.
[18] M. Kimura, O. Sueoka, A. Hamada, M. Takekawa, Y. Itikawa, H. Tanaka, L. Boesten, J. Chem. Phys. 107 (1997) 6616.
[19] J.F. Ying, K.T. Leung, Phys. Rev. A 53 (1996) 1476.
[20] O. Sueoka, M.K. Kawada, M. Kimura, Nucl. Instr. and Meth. 171 (2000) 99.